ACS APPLIED MATERIALS & INTERFACES

Research Article

www.acsami.org

Improving the Quality of GaN Crystals by Using Graphene or Hexagonal Boron Nitride Nanosheets Substrate

Lei Zhang,[†,§] Xianlei Li,[†,§] Yongliang Shao,[†] Jiaoxian Yu,[‡] Yongzhong Wu,[†] Xiaopeng Hao,*[,†] Zhengmao Yin,[†] Yuanbin Dai,[†] Yuan Tian,[†] Qin Huo,[†] Yinan Shen,[†] Zhen Hua,[†] and Baoguo Zhang[†]

[†]State Key Lab of Crystal Materials, Shandong University, Jinan 250100, P. R. China

[‡]Department of Materials Science and Engineering, Qilu University of Technology, Jinan 250353, P. R. China

Supporting Information

ABSTRACT: The progress in nitrides technology is widely believed to be limited and hampered by the lack of high-quality gallium nitride wafers. Though various epitaxial techniques like epitaxial lateral overgrowth and its derivatives have been used to reduce defect density, there is still plenty of room for the improvement of gallium nitride crystal. Here, we report graphene or hexagonal boron nitride nanosheets can be used to improve the quality of GaN crystal using hydride vapor phase epitaxy methods. These nanosheets were directly deposited on the substrate that is used for the epitaxial growth of GaN crystal. Systematic characterizations of the as-obtained crystal show that quality of GaN crystal is greatly improved. The fabricated light-emitting diodes using the as-obtained GaN crystals emit strong electroluminescence under room illumination. This simple yet effective technique is believed to be applicable in metal−organic chemical vapor deposition systems and will find wide applications on other crystal growth.

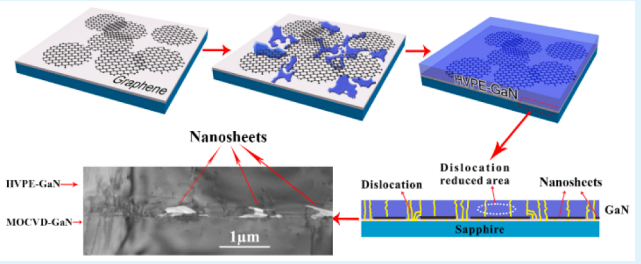

KEYWORDS: *graphene, boron nitride nanosheets, GaN, hydride vapor phase epitaxy, light-emitting diodes*

1. INTRODUCTION

Gallium nitride (GaN) is an important semiconductor material for applications in short wavelength optoelectronics and high-power, high-frequency electronics because of its wide band gap and stability at high temperatures.[1,2] However, because of a lack of native substrates, almost all GaN-based devices are heteroepitaxially grown on foreign substrates, such as sapphire (Al_2O_3), gallium arsenide (GaAs), and silicon.[3−5] Hetero-epitaxial growth produces several stressed layers with a high defect density and with cracking problems due to the large lattice mismatch and difference in thermal expansion coefficient between substrate and layer.[6] The high dislocation density is not conducive to the fabrication of high-performance GaN-based devices with long lifetime. Some low-temperature deposited buffer layer techniques have been used to obtain high-quality GaN crystals, reducing the stress and the dislocation density, and facilitating the removal of the substrate.[7−11] To further improve the quality of GaN epitaxial crystals, epitaxial lateral overgrowth technology has been developed, producing high-quality GaN crystals.[12] However, progress in nitride technology is still inhibited by the lack of high-quality GaN wafers.[13]

Currently two-dimensional (2D) materials have been extensively explored in terms of their properties and applications, mainly because of their excellent properties.[14] Their novel applications in different fields have never ceased to surprise the scientific community.[15] Previously, Kunook Chung et al. reported that a graphene film can be used as a release for mechanically removing a thin-film device from a substrate.[16] Y. Kobayashi et al. reported that hexagonal boron nitride (h-BN) acted as a buffer layer for a nitride film device and enabled the device to be released from the substrate and to be transferred to another different substrate.[17] However, there are few works to investigate the influence of (2D) materials for growing crystal. In this paper, graphene layers and h-BN nanosheets are used as a mask layer to partially block the propagation of defects from the substrate. Clearly, the prime goal of introducing layered materials is to improve the crystal quality rather than function as a releasing layer, which is markedly different from the previous reports.[16,17] This simple yet effective technique can significantly improve the crystalline quality of GaN grown by the hydride vapor phase epitaxy (HVPE) method.

2. RESULTS AND DISCUSSION

The as-obtained GaN epitaxial crystals have a mirrorlike smooth surface. Photographs of GaN crystals grown on metal−organic chemical vapor deposition (MOCVD) systems consisting of graphene nanosheet-coated MOCVD-GaN/Al_2O_3 (GMGA), h-BN nanosheet-coated MOCVD-GaN/Al_2O_3 (h-BNMGA), and MOCVD-GaN/Al_2O_3 (MGA)

Received: September 3, 2014
Accepted: February 9, 2015
Published: February 9, 2015

DOI: 10.1021/am5087775
ACS Appl. Mater. Interfaces 2015, 7, 4504−4510

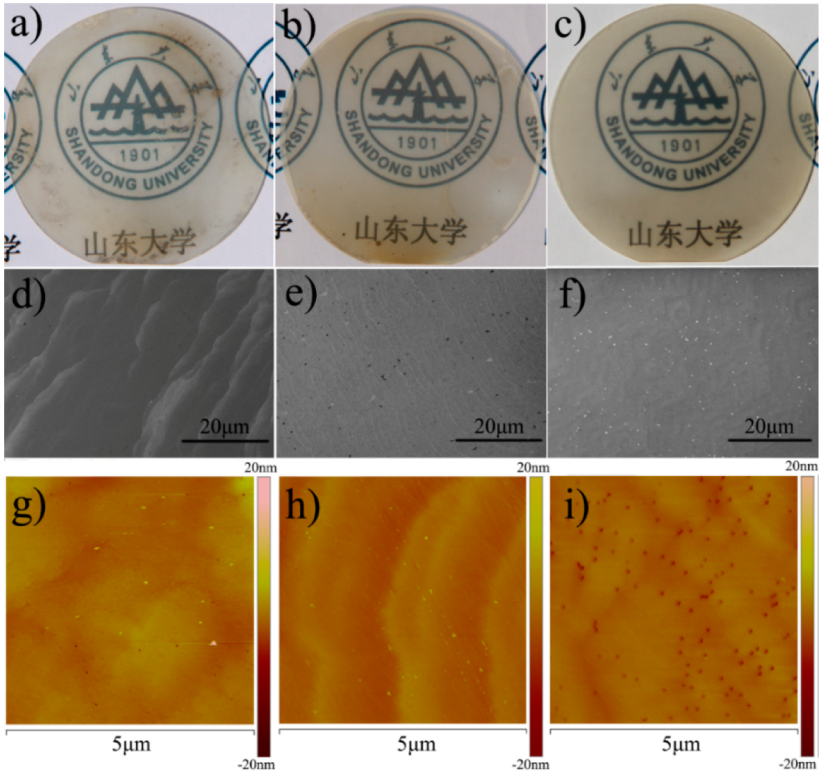

Figure 1. Characterization of GaN crystals. (a–c) photographs of GaN crystal grown on GMGA, h-BNMGA, and MGA templates, respectively; (d–f) SEM images of GaN crystal grown on GMGA,h-BNMGA, and MGA templates, respectively; (g–i) 5 μm × 5 μm AFM images of GaN crystal grown on GMGA, h-BNMGA, and MGA templates, respectively.

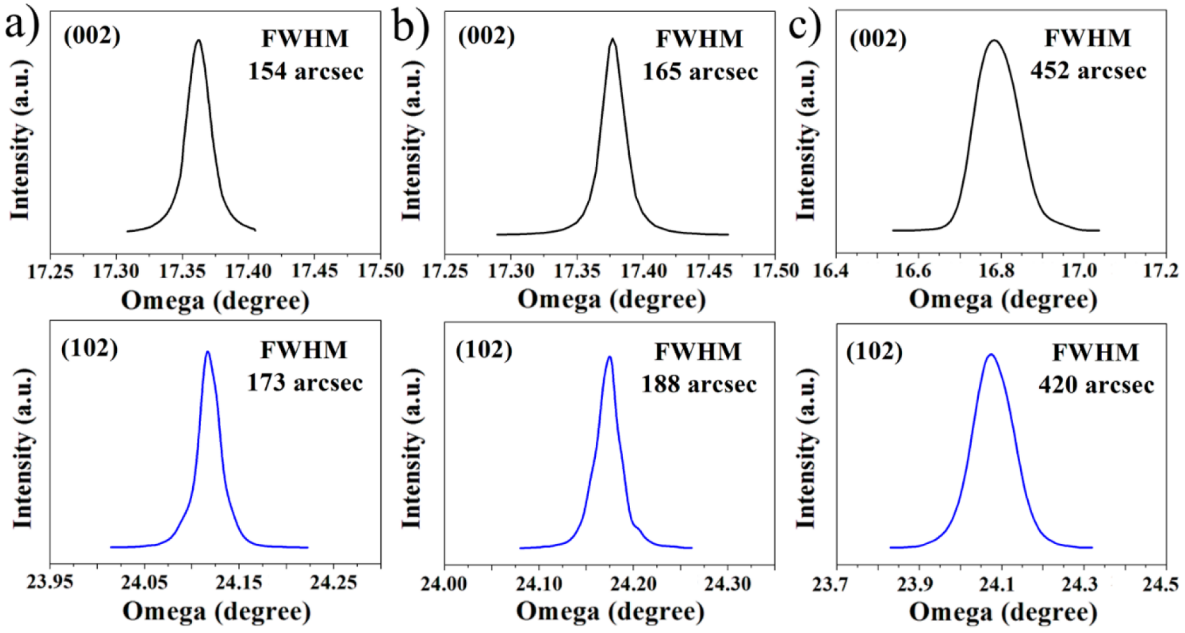

Figure 2. HRXRD rocking curves of GaN crystals on GMGA (a), h-BNMGA (b), and MGA (c) templates (002) ω-scans and (102) ω-scans.

templates are shown in Figure 1a–c. Figure 1d–f shows scanning electron microscopy (SEM) images of the surface morphology of the GaN crystals grown on the GMGA, h-BNMGA, and MGA templates. Atomic force microscopy (AFM) images shown in Figure 1g–i reveal the microstructure of the GaN layers. The root-mean-square (RMS) roughness (5 μm × 5 μm) of the as-obtained GaN crystals grown on the GMGA, h-BNMGA, and MGA templates is ~0.76 nm, 1.21, and 1.74 nm, respectively. Many point defects are observed on the surface of GaN crystals grown on MGA template, which may be caused by edge-type dislocations.[18] In contrast, the point defects are rarely found both on the surfaces of GaN crystals grown on GMGA and h-BNMGA. This directly indicates that the crystal quality of the GaN crystals is considerably improved by using the GMGA and h-BNMGA

DOI: 10.1021/am5087775
ACS Appl. Mater. Interfaces 2015, 7, 4504–4510

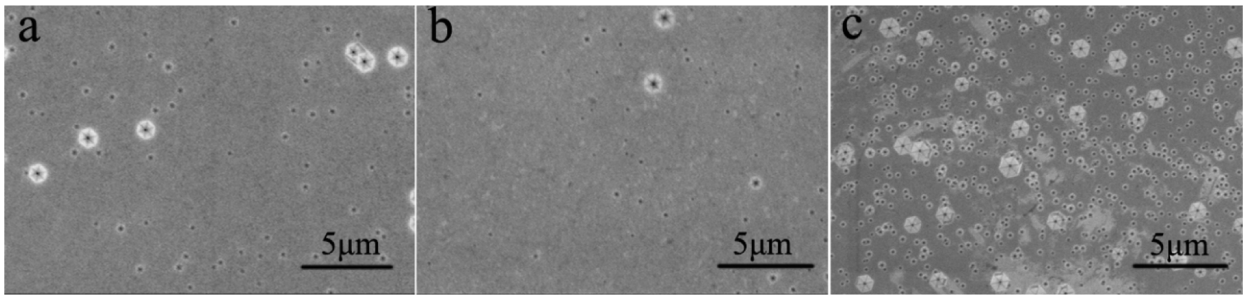

Figure 3. SEM images of etched GaN crystals grown on GMGA (a), BMGA (b), and MGA (c) substrate.

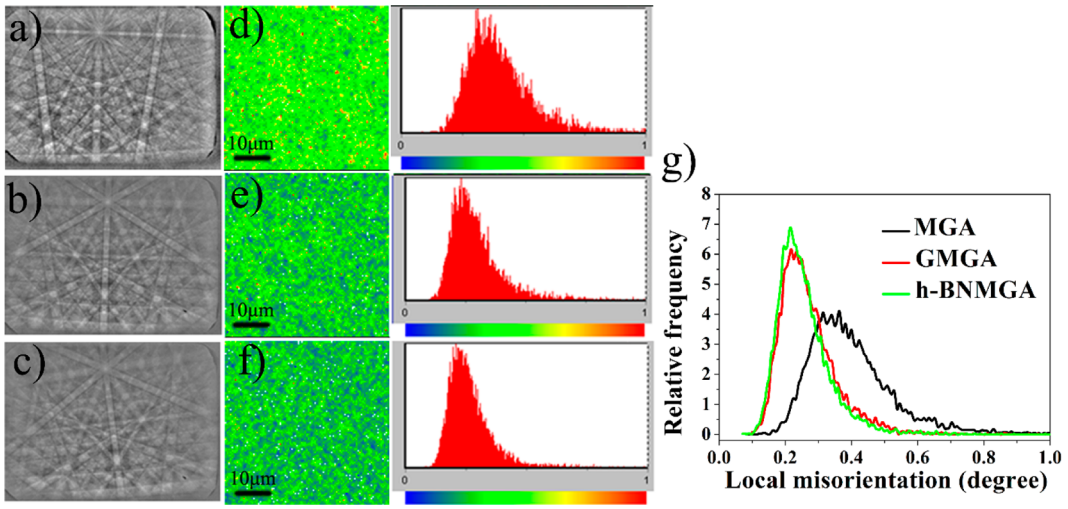

Figure 4. (a–c) EBSD Kikuchi patterns of GaN crystals grown on GMGA, h-BNMGA, and MGA templates. The local misorientation component obtained from EBSD mapping data for GaN crystals grown on (d) MGA, (e) GMGA, and (f) h-BNMGA templates. The misorientation scale is shown, with a variation of up to 1°. (g) The misorientation distribution for GaN crystals grown on GMGA, h-BNMGA, and MGA templates.

template. Moreover, the comparison of the RMS roughness data shows the improvement of the GaN crystal quality.

The crystalline quality of the GaN crystals was characterized by a high-resolution X-ray diffraction (HRXRD) rocking curve. Figure 2 depicts the ω-scan spectra of the (002) symmetry planes and the (102) asymmetry planes of GaN crystals grown on different templates. The full width at half-maximum (FWHM) of the (002) peak is 154, 165, and 452 arcsec for GaN grown on GMGA, h-BNMGA, and MGA templates, respectively. The FWHM of the (102) peak is 173, 188, and 420 arcsec for GaN grown on GMGA, h-BNMGA, and MGA templates, respectively. Previous studies have demonstrated that the screw dislocation density and the edge dislocation density are indirectly represented, respectively, by the FWHM of the HRXRD peaks for the (002) and (102) planes.[19,20] The lower FWHM values of the (002) and (102) peaks of the GaN crystals grown on GMGA and h-BNMGA templates suggest that there are fewer threading dislocations present than with the MGA template.

According to reported references[21−25] and our prior studies,[26,27] we performed etching experiments in an eutectic KOH−NaOH mixture (420 °C, 6 min) to determine the dislocation density in GaN crystals. Figure 3 shows the SEM images of etched GaN crystals grown on GMGA, BMGA, and MGA substrate. The densities of the etching pits in the GaN crystals grown on the GMGA and h-BNMGA templates are ~1.80×10^7 cm^{-2} and 1.09×10^7 cm^{-2}, respectively, less than the value of 1.53×10^8 cm^{-2} in the GaN crystal grown on the MGA template. The results also confirm that the GMGA and h-BNMGA templates effectively reduce the dislocation density in the GaN crystals.

Electron backscatter diffraction (EBSD) is an effective technique for studying the crystal phase, orientation, and lattice strain variations that are typical in semiconducting materials.[28−31] This technique allows us to probe the mechanism of the crystal quality improvement at micrometer level by providing the information on the misorientation distribution of the sample. Figure 4a–c shows the EBSD Kikuchi patterns of GaN crystals grown on (a) GMGA, (b) h-BNMGA, and (c) MGA templates. The high-quality diffraction patterns were collected from the surface, providing orientational indexing of the GaN crystal (a highly oriented crystal structure along the *c*-axis) on these templates. The local misorientation component exhibits small orientation changes on the map, highlighting regions of higher deformation. This component calculates the average misorientation between every pixel and its surrounding pixels and assigns the mean value to the central pixel. Mapping of the small orientation changes provides sufficient detail for quantitative analysis of the crystallographic integrity of GaN. Figure 4 (d–f) shows the local misorientation component obtained from EBSD mapping data for GaN crystals grown on MGA, GMGA, and h-BNMGA templates. It is clear that on the map of crystals grown on the MGA template (d), there are areas colored with a mixture of green and yellow, signifying a 0.2–0.75° orientation change. On the map of crystals grown on the GMGA template (e) and

DOI: 10.1021/am5087775
ACS Appl. Mater. Interfaces 2015, 7, 4504−4510

h-BNMGA template (f), however, the predominantly green and blue color indicates that for almost the entire area, the orientation change is less than 0.5°. Figure 4g shows the misorientation distribution for GaN crystals grown on the GMGA, h-BNMGA, and MGA templates. Compared with the crystals grown on the MGA template, the misorientation distribution widths for the crystals grown on the GMGA and h-BNMGA templates decrease. These results indicate that the crystallographic integrity of the GaN crystal is improved by using GMGA and h-BNMGA templates.

Figure 5a–c shows the SIMS depth profile of the GaN crystals grown on the GMGA, BMGA, and MGA substrates. Table 1 shows the SIMS measurement results for all obtained GaN crystals. As indicated in Table 1, the C concentration in GaN crystal grown on the GMGA template is 1.2×10^{17} cm^{-3}, which is higher than those grown on the BMGA and MGA templates. The C probably came from graphene on the GMGA template. The O concentration in GaN crystal grown on the BMGA templates is more than 1 order of magnitude higher than those grown on the GMGA and MGA templates. This is because O can be easily introduced in the preparing process of hexagonal boron nitride nanosheets.

Raman spectroscopy can provide information about the vibrational states of GaN that are sensitive to crystalline quality and stress. Hexagonal wurtzite GaN has space group C_{6v}^4 with four atoms in the primitive cell. Near $K = 0$, group theory predicts eight sets of phonon modes: $2E_2$, $2A_1$, $2E_1$, and 2B. Only the two E_2 sets, one A_1 set and one E_1 set, are Raman active.[32] The optical modes, which can easily be seen with first-order Raman scattering, consist of a doubly degenerate transverse optical (TO) mode and a single longitudinal optical (LO) mode at a higher frequency.[33] The E_2 phonon frequency gives information on internal stress and crystalline quality. The shift of the E_2 phonon lines observed in Raman measurement is a good indication of the amount of stress in the crystal.[34]

As observed in Figure 6, the E_2 phonon peaks of the GaN crystal grown on the h-BNMGA, GMGA, and MGA templates were observed at 568.066, 568.252, and 568.519 cm^{-1}, respectively. The position of the E_2 (TO) mode of a GaN bulk single crystal (stress-free standard) is taken to be 567.6 cm^{-1}.[35,36] On the basis of this value, we calculate the compressive stress relaxation using the equation[37]

$$\sigma = \frac{\Delta\omega}{4.2}(\mathrm{cm}^{-1}\ \mathrm{GPa}^{-1}) \quad (1)$$

where $\Delta\omega$ is the E_2 phonon peak shift, and σ is the biaxial stress. With these data, it is calculated that the compressive stress that exists in the HVPE GaN crystals grown on the h-BNMGA, GMGA, and MGA templates is ~0.111, 0.155, and 0.219 GPa, respectively. Therefore, stress relaxation of 0.108 and 0.064 GPa is estimated in using the h-BNMGA and GMGA templates.

Combining the above analyses and our experiments on the early stage of GaN crystal growth (see Supporting Information S2), the process of the GaN crystal growth and the mechanism of the quality improvement of the GaN crystal are speculated as follows (a schematic illustration is shown in Figure 7): In the nucleation phase, most nucleation occurs at the interface between the sheet and the substrate along the perimeter of the graphene nanosheets (see Supporting Information S2). And no nucleation or growth occurred on the nanosheets, which is consistent with reports by Kunook Chung[16] et al and by Y. Kobayashi[17] et al. that GaN nucleation does not occur on the basal plane of pristine graphene and h-BN nanosheets. Then these nuclei gradually grow into islands in the lateral

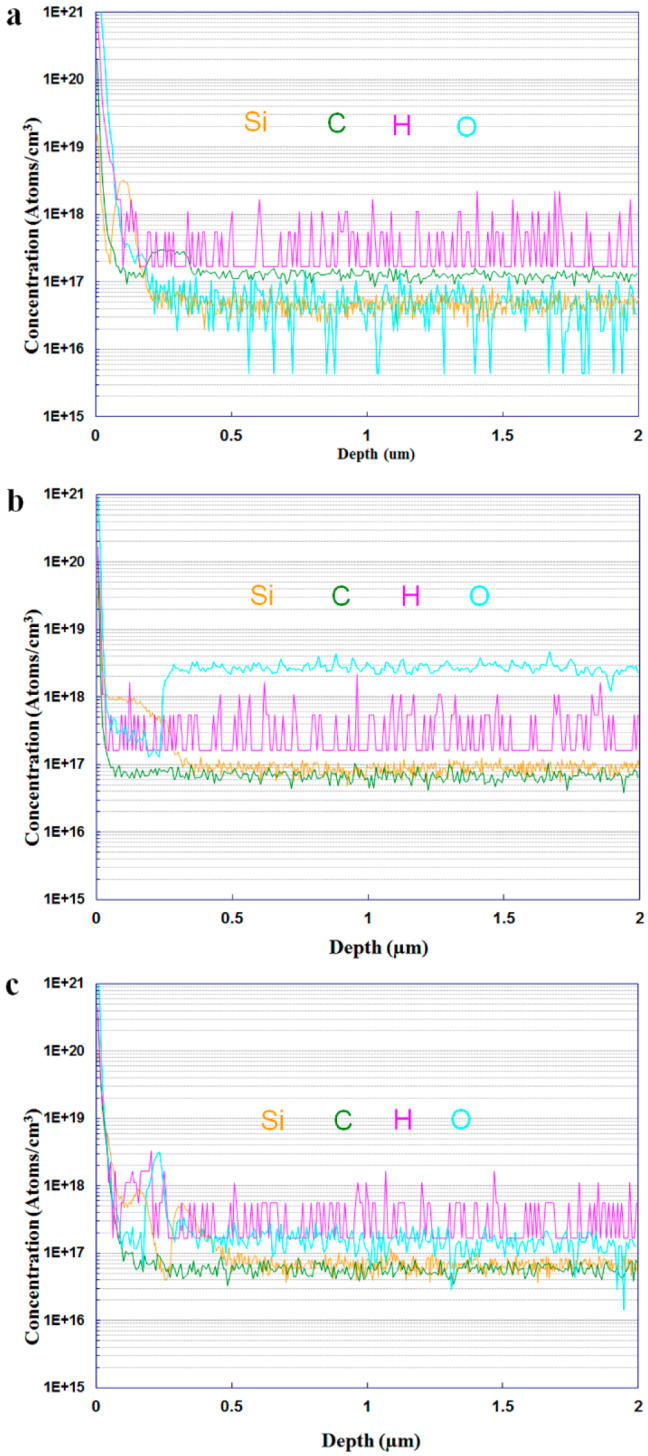

Figure 5. (a–c) The SIMS depth profile of the GaN crystals grown on the GMGA, BMGA, and MGA substrates.

Table 1. SIMS Measurement Results for GaN Crystals Grown on GMGA, BMGA, and MGA Template

sample	C (cm^{-3})	H (cm^{-3})	O (cm^{-3})	Si (cm^{-3})
GMGA	1.2×10^{17}	1.8×10^{17}	5×10^{16}	5×10^{16}
BMGA	7×10^{16}	1.8×10^{17}	3×10^{18}	8×10^{16}
MGA	6×10^{16}	1.8×10^{17}	1.5×10^{17}	7×10^{16}

DOI: 10.1021/am5087775
ACS Appl. Mater. Interfaces 2015, 7, 4504–4510

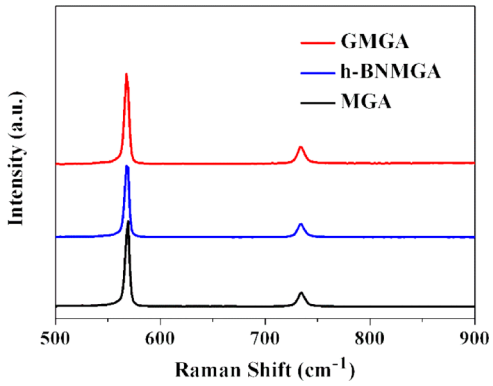

Figure 6. Raman spectra of GaN crystals.

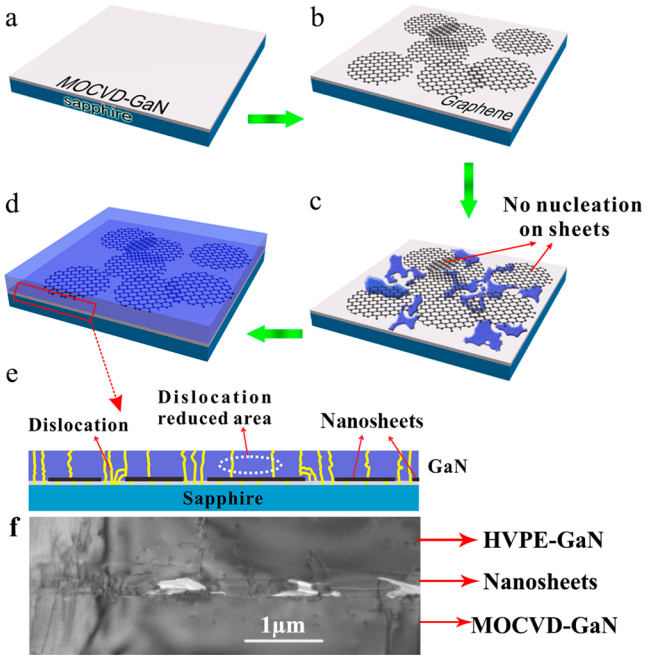

Figure 7. (a–d) Fabrication processes of GaN crystal growth. (e) The mechanism of the quality improvement of the GaN crystal on graphene or h-BN nanosheets coating layers. (f) The cross-sectional TEM bright-field images of GaN grown on h-BNMGA template.

overgrowth way (see Figure 7c). Such lateral epitaxy growth extends over the nanosheets until coalescence of the islands and smoothing occurrence (see Figure 7d). Thus, dislocations in the substrate beneath the nanosheets are blocked and cannot propagate into the lateral epitaxial layer. This growth mode also effectively blocks the propagation of the threading dislocations arising from the MOCVD-GaN substrate (see Figure 7e). Therefore, the as-obtained GaN epitaxial crystals have much lower dislocation density and higher quality. The dislocation annihilation processes caused by the nanosheets were also revealed by the direct cross-sectional transmission electronic microscopy (TEM) observations of the as grown GaN crystal. Figure 7f shows the cross-sectional TEM bright-field images of GaN grown on h-BNMGA template. It shows that the dislocations in the nanosheets area are terminated by h-BN nanosheets, and most of them bend toward the nanosheets area, which leads to a significant reduction in threading dislocation densities. In contrast, threading dislocations from the underlying GaN layer/substrate interface penetrating through the GaN layers in other regions are found. All these findings directly demonstrate that nanosheets can be used to improve the quality of GaN crystals.

High-quality GaN films grown on the GMGA and h-BNMGA substrates can be used to fabricate many optoelectronic devices, such as light-emitting diodes (LEDs) and laser diodes (LDs). We fabricated LEDs as an example of a device application. Figure 8a shows a schematic diagram of the fabrication of GaN LEDs on GMGA and h-BNMGA substrates. The LED structure consists of n-GaN (1 μm), 15 periods of InGaN/GaN multiple-quantum-wells (MQW), p-GaN (200 nm), indium tin oxide (200 nm), and p- and n-type Cr/Au electrodes. The GaN LEDs fabricated on GMGA and h-BNMGA substrates emitted strong blue light under normal room illumination. From the optical microscopy image in Figure 8b, it can be seen that the light emission was fairly uniform over an area of 14 × 18 mil^2 on the GMGA and h-BNMGA substrates. Figure 8c shows the light output power (LOP) curves of GaN-based LEDs on the GMGA, h-BNMGA, and MGA substrates as a function of injection current. The LOP of LEDs on the GMGA, h-BNMGA, and MGA substrates is 47.2, 44.7, and 20.5, respectively, at a forward current of 60 mA. The LOP of LEDs on the GMGA and h-BNMGA substrates is greater than those grown on the MGA substrate by 130.2% and 118.0%, respectively, at 60 mA. The dramatic increase in the LOP of LEDs is attributed to the improvement of cryatlline quality enhanced by 2D nanosheets.[38,39] As shown in Figure 8d, the current–voltage (I–V) curves of LEDs on the GMGA, h-BNMGA, and MGA substrates show good rectifying behavior with a turn-on voltage of 2.6 V. These data indicate that the graphene and h-BN nanosheets cause no degradation of the electrical properties of the LEDs.

3. CONCLUSION

In summary, we have demonstrated that graphene or h-BN nanosheets can be used to significantly enhance the quality of GaN crystals. Introducing graphene and h-BN nanosheets on substrates can effectively block the thread dislocation propagating, create lateral overgrowth along the circumference of sheets, and reduce the nucleation of GaN. The performance of LEDs fabricated using high-quality GaN films grown on GMGA and h-BNMGA substrates improved considerably. The improvement is independent of the chemical components of the nanosheets, although the degree of improvement is different from type to type. Therefore, we expect that by using this technique, other nanosheets such as WS_2 and MoS_2 can also be used to improve the quality of GaN crystals.

4. METHODS

Multilayered graphene nanosheets and h-BN nanosheets were prepared according to previously reported methods.[40,41] The 2D nanosheets were directly deposited onto a variety of substrates by the spin-coating method. With this technique, graphene- or h-BN nanosheet-coated MOCVD-GaN/Al_2O_3 (GMGA and h-BNMGA, respectively) templates were fabricated. A template with a 5 μm GaN layer grown by MOCVD on an Al_2O_3 substrate was employed as the starting substrate. The graphene and h-BN solutions were spin-coated onto the substrate and then dried in a vacuum oven at 80 °C for 24 h.

The GMGA and h-BNMGA templates were mounted in the HVPE reactor to grow GaN layers. Ga and NH_3 were used as gallium and nitrogen sources. HCl gas was reacted with liquid Ga at 820 °C to form GaCl, which was transported to the growth zone of the reactor and reacted with NH_3 at 1030 °C to form the GaN deposition on the

DOI: 10.1021/am5087775
ACS Appl. Mater. Interfaces 2015, 7, 4504–4510

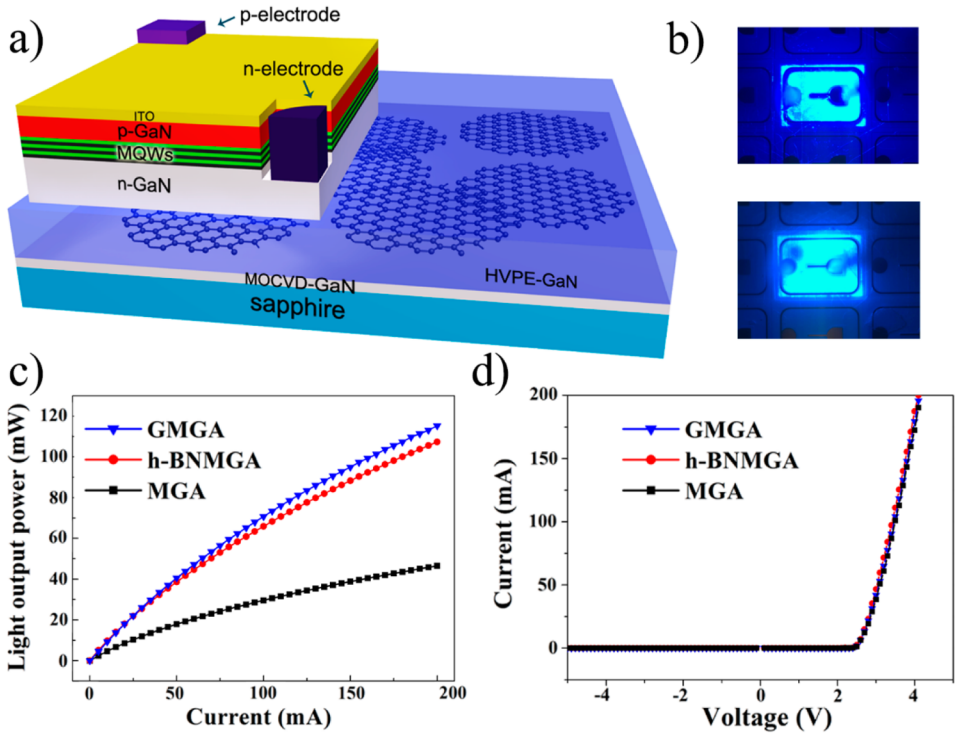

Figure 8. (a) Fabrication of LEDs on GMGA and h-BNMGA substrates. (b) Optical images of light emission from as-fabricated LED on the GMGA and h-BNMGA substrates. (c) The light output power curves of the GaN-based LEDs on GMGA, h-BNMGA, and MGA substrates as a function of injection current. (d) Current–voltage curves of the LEDs on GMGA, h-BNMGA, and MGA substrates.

substrate. Nitrogen was used as the carrier gas. The reactor pressure was kept near atmospheric pressure. The NH_3 flow rate was held within the range of 800–1000 mL/min, while the HCl flow rate was 10–20 mL/min. The growth rate was controlled within the range of 10–30 μm/h. The thickness of the resulting GaN layer was ~40 μm.

The GaN-based LEDs with the size of 14 × 18 mil^2 were fabricated by conventional process. The GaN-based LED wafer was grown on the GMGA and h-BNMGA substrates by MOCVD. The LED chip structure consists of GMGA or h-BNMGA substrates (440 μm), undoped GaN (u-GaN, 2 μm), n-GaN (1 μm), 15 periods of InGaN/GaN multiple-quantum-wells (MQWs), p-GaN (200 nm), indium tin oxide (200 nm), and p- and n-type Cr/Au electrodes.

SEM images were taken with a Hitachi S-4800 field emission microscope equipped with a Horiba EX-450 energy-dispersive X-ray spectroscopy (EDS) attachment. AFM (Digital Instrument Dimension 3100) was used to investigate surface morphology. Defect selective etching in molten KOH–NaOH eutectic was performed to reveal dislocations threading to the growth surface of GaN crystals. The Raman spectra of the samples were obtained with a LabRAM HR system of Horiba Jobin Yvon at room temperature using a 532 nm solid-state laser as the excitation source. The TEM specimens of the GaN crystal were prepared by conventional method of mechanical polishing followed by ion milling. The sample was imaged in FEI Tecnai TF-20 FEG/TEM operated at 200 kV. The crystalline quality of the GaN crystals was characterized by HRXRD using symmetrical (002) and asymmetrical (102) reflections. Background impurity levels of GaN crystals were measured by SIMS. The crystal structure and orientation was characterized with an EBSD system (Oxford Instruments INCA Crystal EBSD system, Nordlys EBSD Detector, and HKL CHANNEL5 software) in the FE-SEM. The EBSD measurements were carried out at 20 kV with a working distance of 20 mm and a sample tilt of 70°.

■ ASSOCIATED CONTENT

Supporting Information

SEM and TEM characterization of graphene and boron nitride nanosheets. GaN crystal growth process. Control experiments on GaN crystals directly grown on sapphire substrate. Electroluminescence characterization of the fabricated LEDs. This material is available free of charge via the Internet at http://pubs.acs.org.

■ AUTHOR INFORMATION

Corresponding Author

*E-mail: xphao@sdu.edu.cn.

Author Contributions

§These authors (L.Z. and X.L.) contributed equally to this work.

Notes

The authors declare no competing financial interest.

■ ACKNOWLEDGMENTS

This work was supported by the National Natural Science Foundation of China (Grant Nos. 51321091 and 51402171), IIFSDU, China Postdoctoral Science Foundation funded project (2012M521331, 2014T70634), and the Special Fund from Postdoctoral Innovation Research Program of Shandong Province (201203062). We especially thank Dr. R. I. Boughton, Prof. Em. at Bowling Green State Univ., for linguistic help.

■ REFERENCES

(1) Ehrentraut, D.; Sitar, Z. Advances in Bulk Crystal Growth of AlN and GaN. *MRS Bull.* **2009**, *34*, 259–265.

(2) Jia, H. Q.; Guo, L. W.; Wang, W. X.; Chen, H. Recent Progress in GaN-Based Light-Emitting Diodes. *Adv. Mater.* **2009**, *21*, 4641–4646.

DOI: 10.1021/am5087775
ACS Appl. Mater. Interfaces 2015, 7, 4504–4510

(3) Hemmingsson, C.; Paskov, P. P.; Pozina, G.; Heuken, M.; Schineller, B.; Monemar, B. Hydride Vapour Phase Epitaxy Growth and Characterization of Thick GaN using a Vertical HVPE Reactor. *J. Cryst. Growth* **2007**, *300*, 32−36.
(4) Motoki, K.; Okahisa, T.; Nakahata, S.; Matsumoto, N.; Kimura, H.; Kasai, H.; Takemoto, K.; Uematsu, K.; Ueno, M.; Kumagai, Y.; Koukitu, A.; Seki, H. Growth and Characterization of Freestanding GaN Substrates. *J. Cryst. Growth* **2002**, *237*−*239*, 912−921.
(5) Zhang, J. X.; Qu, Y.; Chen, Y. Z.; Uddin, A.; Yuan, S. Structural and Optical Characterization of GaN Epilayers Grown on Si(1 1 1) Substrates by Hydride Vapor-Phase Epitaxy. *J. Cryst. Growth* **2005**, *282*, 137−142.
(6) Hemmingsson, C.; Pozina, G. Optimization of Low Temperature GaN Buffer Layers for Halide Vapor Phase Epitaxy Growth of Bulk GaN. *J. Cryst. Growth* **2013**, *366*, 61−66.
(7) Valcheva, E.; Paskova, T.; Tungasmita, S.; Persson, P. O. Å.; Birch, J.; Svedberg, E. B.; Hultman, L.; Monemar, B. Interface Structure of Hydride Vapor Phase Epitaxial GaN Grown with High-temperature Reactively Sputtered AlN Buffer. *Appl. Phys. Lett.* **2000**, *76*, 1860.
(8) Detchprohm, T.; Hiramatsu, K.; Amano, H.; Akasaki, I. Hydride Vapor Phase Epitaxial Growth of a High Quality GaN Film using a ZnO Buffer Layer. *Appl. Phys. Lett.* **1992**, *61*, 2688.
(9) Oshima, Y.; Eri, T.; Shibata, M.; Sunakawa, H.; Usui, A. Fabrication of Freestanding GaN Wafers by Hydride Vapor-phase Epitaxy with Void-Assisted Separation. *Phys. Status Solidi A* **2002**, *194*, 554−558.
(10) Chao, C. L.; Chiu, C. H.; Lee, Y. J.; Kuo, H. C.; Liu, P.-C.; Tsay, J. D.; Cheng, S. J. Freestanding High Quality GaN Substrate by Associated GaN Nanorods Self-Separated Hydride Vapor-Phase Epitaxy. *Appl. Phys. Lett.* **2009**, *95*, 051905.
(11) Akasaki, I. Progress in Crystal Growth of Nitride Semiconductors. *J. Cryst. Growth* **2000**, *221*, 231−239.
(12) Beaumont, B.; Vennéguès, P.; Gibart, P. Epitaxial Lateral Overgrowth of GaN. *Phys. Status Solidi B* **2001**, *227*, 1−43.
(13) Bockowski, M. Bulk Growth of Gallium Nitride: Challenges and Difficulties. *Cryst. Res. Technol.* **2007**, *42*, 1162−1175.
(14) Xu, M.; Liang, T.; Shi, M.; Chen, H. Graphene-Like Two-Dimensional Materials. *Chem. Rev.* **2013**, *113*, 3766.
(15) Butler, S. Z.; Hollen, S. M.; Cao, L. Y.; Cui, Y.; Gupta, J. A.; Gutiérrez, H. R.; Heinz, T. F.; Hong, S. S.; Huang, J.; Ismach, A. F.; Halperin, E. J.; Kuno, M.; Plashnitsa, V. V.; Robinson, R. D.; Ruoff, R. S.; Salahuddin, S.; Shan, J.; Shi, L.; Spencer, M. G.; Terrones, M.; Windl, W.; Goldberger, J. E. Progress, Challenges, and Opportunities in Two-Dimensional Materials beyond Graphene. *ACS Nano* **2013**, *7*, 2898.
(16) Chung, K.; Lee, C. H.; Yi, G. C. Transferable GaN Layers Grown on ZnO-Coated Graphene Layers for Optoelectronic Devices. *Science* **2010**, *330*, 655−657.
(17) Kobayashi, Y.; Kumakura, K.; Akasaka, T.; Makimoto, T. Layered Boron Nitride as a Release Layer for Mechanical Transfer of GaN-Based Devices. *Nature* **2012**, *484*, 223−227.
(18) Hino, T.; Tomiya, S.; Miyajima, T.; Yanashima, K.; Hashimoto, S.; Ikeda, M. Characterization of Threading Dislocations in GaN Epitaxial Layers. *Appl. Phys. Lett.* **2000**, *76*, 3421−3423.
(19) Heinke, H.; Kirchner, V.; Einfeldt, S.; Hommel, D. X-Ray Diffraction Analysis of the Defect Structure in Epitaxial GaN. *Appl. Phys. Lett.* **2000**, *77*, 2145−2147.
(20) Ko, H. J.; Yao, T.; Chen, Y.; Hong, S. K. Investigation of ZnO Epilayers Grown under Various Zn/O Ratios by Plasma-Assisted Molecular-Beam Epitaxy. *J. Appl. Phys.* **2002**, *92*, 4354−4360.
(21) Weyher, J. L.; Lazar, S.; Macht, L.; Liliental-Weber, Z.; Molnar, R. J.; Müller, S.; Sivel, V. G. M.; Nowak, G.; Grzegory, I. Orthodox Etching of HVPE-Grown GaN. *J. Cryst. Growth* **2007**, *305*, 384−392.
(22) Weyher, J. L.; Ashraf, H.; Hageman, P. R. Reduction of Dislocation Density in Epitaxial GaN Layers by Overgrowth of Defect-Related Etch Pits. *Appl. Phys. Lett.* **2009**, *95*, 031913.
(23) Meissner, E.; Schweigard, S.; Friedrich, J.; Paskova, T.; Udwary, K.; Leibiger, G.; Habel, F. Cathodoluminescence Imaging for the Determination of Dislocation Density in Differently Doped HVPE GaN. *J. Cryst. Growth* **2012**, *340*, 78−82.
(24) Yoshida, K.; Aoki, K.; Fukuda, T. High-Temperature Acidic Ammonothermal Method for GaN Crystal Growth. *J. Cryst. Growth* **2014**, *393*, 93−97.
(25) Sochacki, T.; Bryan, Z.; Amilusik, M.; Bobea, M.; Fijalkowski, M.; Bryan, I.; Lucznik, B.; Collazo, R.; Weyher, J. L.; Kucharski, R.; Grzegory, I.; Bockowski, M.; Sitar, Z. HVPE-GaN Grown on MOCVD-GaN/sapphire Template and Ammonothermal GaN Seeds: Comparison of Structural, Optical, and Electrical Properties. *J. Cryst. Growth* **2014**, *394*, 55−60.
(26) Zhang, L.; Shao, Y. L.; Wu, Y. Z.; Hao, X. P.; Chen, X. F. Characterization of Dislocation Etch Pits in HVPE-Grown GaN using Different Wet Chemical Etching Methods. *J. Alloys Compd.* **2010**, *504*, 186−191.
(27) Tian, Y.; Zhang, L.; Wu, Y. Z.; Shao, Y. L.; Dai, Y. B.; Zhang, H. D.; Wei, R. S.; Hao, X. P. Characterization of Dislocations in MOCVD-Grown GaN using a High Temperature Annealing Method. *CrystEngComm* **2014**, *16*, 2317−2322.
(28) Chierchia, R.; Böttcher, T.; Heinke, H.; Einfeldt, S.; Figge, S.; Hommel, D. Microstructure of Heteroepitaxial GaN Revealed by X-Ray Diffraction. *J. Appl. Phys.* **2003**, *93*, 8918.
(29) Shao, Y. L.; Dai, Y. B.; Hao, X. P.; Wu, Y. Z.; Zhang, L.; Zhang, H. D.; Tian, Y. EBSD Crystallographic Orientation Research on Strain Distribution in Hydride Vapor Phase Epitaxy GaN Grown on Patterned Substrate. *CrystEngComm* **2013**, *15*, 7965−7969.
(30) Wilkinson, A. J.; Moldovan, G.; Britton, T. B. Direct Detection of Electron Backscatter Diffraction Patterns. *Phys. Rev. Lett.* **2013**, *111*, 065506.
(31) Trager-Cowan, C.; Sweeney, F.; Trimby, P. W.; Day, A. P.; Gholinia, A.; Schmidt, N. H.; Parbrook, P. J.; Wilkinson, A. J.; Watson, I. M. Electron Backscatter Diffraction and Electron Channeling Contrast Imaging of Tilt and Dislocations in Nitride Thin Films. *Phys. Rev. B* **2007**, *75*, 085301.
(32) Siegle, H.; Kaczmarczyk, G.; Filippidis, L.; Litvinchuk, A. P.; Hoffmann, A.; Thomsen, C. Zone-Boundary Phonons in Hexagonal and Cubic GaN. *Phys. Rev. B* **1997**, *55*, 7000.
(33) Cardona, M. In *Light Scattering in Solids II;* Cardona, M., Güntherodt, G., Eds.; Springer: Amsterdam, Netherlands, 1982; Chapter 2, pp 19−178.
(34) Hartono, H.; Soh, C. B.; Chow, S. Y.; Chua, S. J.; Fitzgerald, E. A. Reduction of Threading Dislocation Density in GaN Grown on Strain Relaxed Nanoporous GaN Template. *Appl. Phys. Lett.* **2007**, *90*, 171917.
(35) Davydov, V. Y.; Kitaev, Yu. E.; Goncharuk, I. N.; Smirnov, A. N.; Graul, J.; Semchinova, O.; Uffmann, D.; Smirnov, M. B.; Mirgorodsky, A. P.; Evarestov, R. A. Phonon Dispersion and Raman Scattering in Hexagonal GaN and AlN. *Phys. Rev. B* **1998**, *58*, 12899.
(36) Lu, J. Y.; Wang, Z. J.; Deng, D. M.; Wang, Y.; Chen, K. J.; Lau, K. M.; Zhang, T. Y. Determining Phonon Deformation Potentials of Hexagonal GaN with Stress Modulation. *J. Appl. Phys.* **2010**, *108*, 123520.
(37) Kisielowski, C. Strain-Related Phenomena in GaN Thin Films. *Phys. Rev. B* **1996**, *54*, 17745.
(38) Long, H.; Wei, Y.; Yu, T. J.; Wang, Z.; Jia, C. Y.; Yang, Z. J.; Zhang, G. Y.; Fan, S. H. High Quality GaN Epilayers Grown on Carbon Nanotube Patterned Sapphire Substrate by Metal-Organic Vapor Phase Epitaxy. *CrystEngComm* **2012**, *14*, 4728−4731.
(39) Long, H.; Wei, Y.; Yu, T. J.; Wang, Z.; Jia, C. Y.; Yang, Z. J.; Zhang, G.; Fan, S. S. Modulating Lateral Strain in GaN-Based Epitaxial Layers by Patterning Sapphire Substrates with Aligned Carbon Nanotube Films. *Nano Res.* **2012**, *5*, 646−653.
(40) Xu, J. L.; L. Li, X.; Wu, Y. Z.; Hao, X. P.; He, J. L.; Yang, K. J. Graphene Saturable Absorber Mirror for Ultra-Fast-Pulse Solid-State Laser. *Opt. Lett.* **2011**, *36*, 1948−1950.
(41) Li, X. L.; Hao, X. P.; Zhao, M. W.; Wu, Y. Z.; Yang, J. X.; Tian, Y. P.; Qian, G. D. Exfoliation of Hexagonal Boron Nitride by Molten Hydroxides. *Adv. Mater.* **2013**, *25*, 2200−2204.

DOI: 10.1021/am5087775
ACS Appl. Mater. Interfaces 2015, 7, 4504−4510